Clim Dyn (2010) 35:29–43
DOI 10.1007/s00382-009-0625-5

A multi-model approach to the Atlantic Equatorial mode: impact on the West African monsoon

T. Losada · B. Rodríguez-Fonseca · S. Janicot · S. Gervois · F. Chauvin · P. Ruti

Received: 23 December 2008 / Accepted: 25 June 2009 / Published online: 22 July 2009

Abstract This paper is focused on the West African anomalous precipitation response to an Atlantic Equatorial mode whose origin, development and damping resembles the observed one during the last decades of the XXth century. In the framework of the AMMA-EU project, this paper analyses the atmospheric response to the Equatorial mode using a multimodel approach with an ensemble of integrations from 4 AGCMs under a time varying Equatorial SST mode. The Guinean Gulf precipitation, which together with the Sahelian mode accounts for most of the summer West African rainfall variability, is highly coupled to this Equatorial Atlantic SST mode or Atlantic Niño. In a previous study, done with the same models under 1958–1997 observed prescribed SSTs, most of the models identify the Equatorial Atlantic SST mode as the one most related to the Guinean Gulf precipitation. The models response to the positive phase of equatorial Atlantic mode (warm SSTs) depicts a direct impact in the equatorial Atlantic, leading to a decrease of the local surface temperature gradient, weakening the West African Monsoon flow and the surface convergence over the Sahel.

Keywords West African Monsoon · Tropical Atlantic variability · Tropical teleconnections

This paper is a contribution to the special issue on West African Climate, consisting of papers from the African Multidisciplinary Monsoon Analysis (AMMA) and West African Monsoon Modeling and Evaluation (WAMME) projects, and coordinated by Y. Xue and P. M. Ruti.

T. Losada (✉) · B. Rodríguez-Fonseca
Universidad Complutense de Madrid, Madrid, Spain
e-mail: tldoval@fis.ucm.es

S. Janicot · S. Gervois
LOCEAN/IPSL, CNRS, Université Pierre et Marie Curie, Paris, France

F. Chauvin
GAME/CNRM, Météo-France/CNRS, Toulouse, France

P. Ruti
Progetto Speciale Clima Globale, Ente Nazionale per le NuoveTecnologie, l'Energia e l'Ambiente, Rome, Italy

1 Introduction

The first mode of variability of the Tropical Atlantic ocean is the well known *Equatorial mode* or *Atlantic Niño*, which peaks in summer and it is characterized by anomalous SST at the eastern equatorial Atlantic basin and the displacement of the convective region southward and eastward, (Zebiak 1993).

It has been shown by several studies how this mode affects Subsaharan summer rainfall. In this way, the well-known dipole between Sahelian and Gulf of Guinea (GG) precipitation (Janicot 1992; Rowell et al. 1995; Ward 1998) has been related to Tropical Atlantic variability; Janicot et al. (1998), Vizy and Cook (2002) and Paeth and Friederichs (2004) among others have described how above normal SSTs in the GG are related to positive precipitation anomalies along the coast of the GG, and negative precipitation anomalies over the Sahelian area. Some of these studies found the southward shift of the tropical rainbelt as the responsible of the dipolar response of the precipitation (Janicot et al. 1998), while others (Shinoda and Kawamura 1994; Vizy and Cook 2002) point to other dynamical aspects as the crucial factor in this precipitation response.

Vizy and Cook (2002) have reproduced the dipolar response to SST anomalies in the Tropical Atlantic Ocean using a Mesoscale climate model (MCM). However, some

simulations performed with Atmospheric general circulation models (AGCM) were not able to produce the same response (Vizy and Cook 2001; Giannini et al. 2005).

Several papers describe how the presence of the dipole of anomalous precipitation over West Africa depends on the satisfaction of the inertial instability criteria (Nicholson 2009; Nicholson and Webster 2007). The criteria are satisfied in years where the Monsoon is strong (wet Sahelian years); these years are also characterized by a strong surface westerly jet that enhances the horizontal and vertical shear, leading to a northward displacement of the AEJ. The development of the westerly jet is directly linked to the cross-equatorial pressure gradient and thus, indirectly to the EM SST pattern (Nicholson and Webster 2007).

As it was pointed by Janicot et al. (2001) the relation between the Subsaharan summer rainfall and SST involves different oceanic basins at different time periods so a first problem found in the above mentioned studies is the use observations including the dry and wet Sahelian sequences in the same analysis and thus, different oceanic influences coexisting with the Equatorial mode. Thus, a more realistic analysis of the mode, in relation with a more homogeneous time period is needed.

Recent studies of Polo et al. (2008) and García-Serrano et al. (2008) update the description of the origin, development, and damping of the Equatorial mode in relation to its direct influence on the Guinean Gulf precipitation. The former work describes the Equatorial mode as a time-evolving SST pattern in relation to the anomalous African rainfall for the period 1979–2001. The Equatorial mode is a tropical Atlantic basin scale mode in which the anomalous SSTs start at the Angola/Benguela region, propagate westward and northward, up to the equatorial band, and damp in the western part of the equatorial basin. García-Serrano et al. (2008) describe the associated precipitation, and how the convection follows the anomalous SST forcing, influencing on the Walker Atlantic branch.

Nevertheless, the dynamics associated to the precipitation response to the mode described in Polo et al. (2008) have not been studied and model effort needs to be made in order to analyze the isolated impact of this SST pattern. This will be one of the points to be addressed in the paper.

The present paper first evaluates the skill of four different models to simulate the atmospheric dynamics associated to the WAM. Then we study the models response to the tropical forcing associated with the Atlantic Niño mode, from a local point of view (influence on the WAM).

An important novelty of this paper is that it treats the Equatorial mode as a continuous mode, taking into account its whole evolution, and maximizing its covariability with West African rainfall. This differs from other modeling studies, that either proposed simulations with a July–September (JAS) mean pattern (Kucharski et al. 2009), or define an idealized SST anomalous pattern (Vizy and Cook 2001). Also, the study covers the period from 1979 to 2005, just after the so-called "climate shift" of the late 1970s (Miller et al. 1994; Cane et al. 1997), a feature that will allow us to investigate the importance of the Atlantic Niño in the Sahel dry period.

This study is divided into four sections. In Sect. 2 we describe the experiments and models used, as well as the observational data. The results of the study are presented in Sect. 3. In Sect. 3.1 we describe the models ability to reproduce the WAM climatology. The models responses to the Equatorial mode over West Africa are described in Sect. 3.2. Finally Sect. 4 provides a discussion of the results and the conclusions of the study.

2 Methodology and data

In order to study the atmospheric response to the Equatorial mode, four different models have been used in a multi-model set of idealized experiments. The models are forced with the leading seasonally varying anomalous tropical Atlantic SST pattern coupled to the Guinean Gulf region and described in Polo et al. (2008). The AGCM used are: ARPEGE (Déqué et al. 1994), ECHAM-4 (Roeckner et al. 1996), LMDZ (Hourdin et al. 2006) and UCLA (Ritcher et al. 2008). The main characteristics of the models analysed in this study are presented in Table 1.

First, a 10-year long control run with climatological Reynolds (Smith and Reynolds 2004) SSTs averaged from 1979 to 2005 was performed by each of the models. This simulation is used to study the models skill in simulating the WAM season; so the mean summer (JAS) fields of the control runs are analyzed and compared with the observations. The observed data used to evaluate the simulations are: the monthly CPC merged analysis of precipitation (CMAP, Xie and Arkin 1997), and the monthly atmospheric reanalysis from ERA40 (Uppala et al. 2005) averaged from 1979 to 2002.

Table 1 Models description

Label	AGCM	Vertical levels	Resolution (lon-lat)
ARPEGE	ARPEGE V3	45	T63, approx. 2.80 × 2.80
ECHAM4	ECHAM 4	19	T30, approx. 3.75 × 3.75
LMDZ	LMDZ 4	19	96 × 71 approx. 3.75 × 2.50
UCLA	UCLA 7.3	29	2.50 × 2.00

Then, two sets of 10-member ensemble simulations, in which an anomalous pattern in the tropical Atlantic has been superposed to the climatological SST, were run from April to September. In the first experiment a positive anomaly has been added to the climatology, while in the second experiment the same anomaly has been subtracted to the climatology; thus, we will refer to these simulations as EMP and EMN respectively. The different response between EMP and EMN will allow us to check the linearity of the response to the anomalous pattern.

To compose the boundary conditions for the sensitivity experiments has been a meticulous task. In the framework of the AMMA-EU project it was decided to carefully define a set of idealized SST anomalies based on the modes of co-variability between worldwide SSTs and African precipitations. Thus, by calculating these patterns for each influencing oceanic basin, we expect to deduce the respective contributions of each of them on the WAM precipitations. To do this, one of the most important requirements was to define simple, realistic and physically coherent SST patterns. In relation to the Atlantic influence, we decided to consider the expansion coefficient of the leading EMCA mode between precipitation and SST described in Polo et al. (2008). This mode shows strong positive links between the GG rainfall and the spring to summer evolution of the Equatorial mode or Atlantic Niño. In order to introduce some physical considerations in the SST patterns definitions, a SST composite was constructed by averaging years for which the phasing between SST and African precipitation was maximal. Technically, they have been computed chosen those years (within the period 1979–2001) in which the SST and June–September precipitation expansion coefficients were higher than 1 standard deviation and those in which the expansion coefficients were less that -1 standard deviation. In the case of the Equatorial mode, the positive selected years were 1984, 1987, 1988, 1989, 1998, 1999; and the negative ones were 1982, 1983, 1992, 1997. In order to amplify the SST signals to force the models, we have chosen to compute the difference between the composite positive and the composite negative SST anomalies to define the composite positive phase, and vice versa for the negative phase. Then positive and negative phases are symmetric.

Figure 1 depicts the anomalous SST pattern used in EMP. It shows an anti-clockwise propagation of positive anomalies from 20°S to the equator, like in Polo et al. (2008) and also in Robertson et al. (2003). The amplitude of the SST signal is at the same level as in Vizy and Cook (2002).

The anomalous response to the Equatorial mode will be computed by subtracting the CONTROL response to the EMP and EMN responses. A test t of equal means (von Storch and Zwiers 1999) at 95% of confidence level will be applied to the results in order to assess the significance of the response.

3 Results

3.1 Models WAM climatology

In this section we analyze the reliability of the models to reproduce the main characteristics of the West African rainy season.

The monsoon onset has been defined as the abrupt shift of the rainfall belt during the end of June (Sultan and Janicot 2000) and is apparent in the 5-day mean evolution of the precipitation averaged between 10°W–10°E for all the models (Fig. 2). The four climatologies show a maximum of precipitation located around 3–6°N during June, followed by a second maximum at 9–12°N in August. There is an abrupt change in the slope of the diagrams in Fig. 2 at the end of June that can be identified as the monsoon onset, in accordance with Sultan and Janicot (2003) that situate the onset mean date on the 24th of June.

Figure 3 shows the precipitation averaged on JAS for the 4-models control runs and the observations (CMAP). All the models capture the three maximums of precipitation observed in the African rainy belt during summer (over Sierra Leona, Cameroon, and Sudan areas). The location of the maximums is well simulated by LMDZ and ARPEGE, while it is placed too far north in ECHAM-4 and especially in UCLA. The amplitude of the rainfall maximums is higher than the observed in UCLA model, while ECHAM-4 and ARPEGE show lower amounts than CMAP. The tropical rainfall belt is too width in UCLA climatology and too narrow in LMDZ and ECHAM-4. Finally, the maximum of precipitation over sea is not well reproduced by all the models except by UCLA, whilst all the models present a maximum of precipitation over the western flank of the tropical belt, that is not present in the observations. These differences in the tropical rainfall belt, and in the associated surface wind convergence (Fig. 4) could have a determinant influence when analyzing the global impacts of the Equatorial mode associated anomalous rainfall.

Some important features controlling the WAM are the inter-hemispheric pressure gradient, the Saharan heat low, the surface flow and the upper and middle tropospheric jets. Figure 4 represents the JAS surface winds and mean sea level pressure (MSLP). The Saharan heat low, located around 20°N inland, controls part of the monsoon winds variability as described in Sultan and Janicot (2003). Its location during JAS is well simulated by all the models, although LMDZ low is placed a bit too far south. The amplitude of the heat low is lower in ECHAM-4 than in ERA40, and somehow higher in ARPEGE and LMDZ.

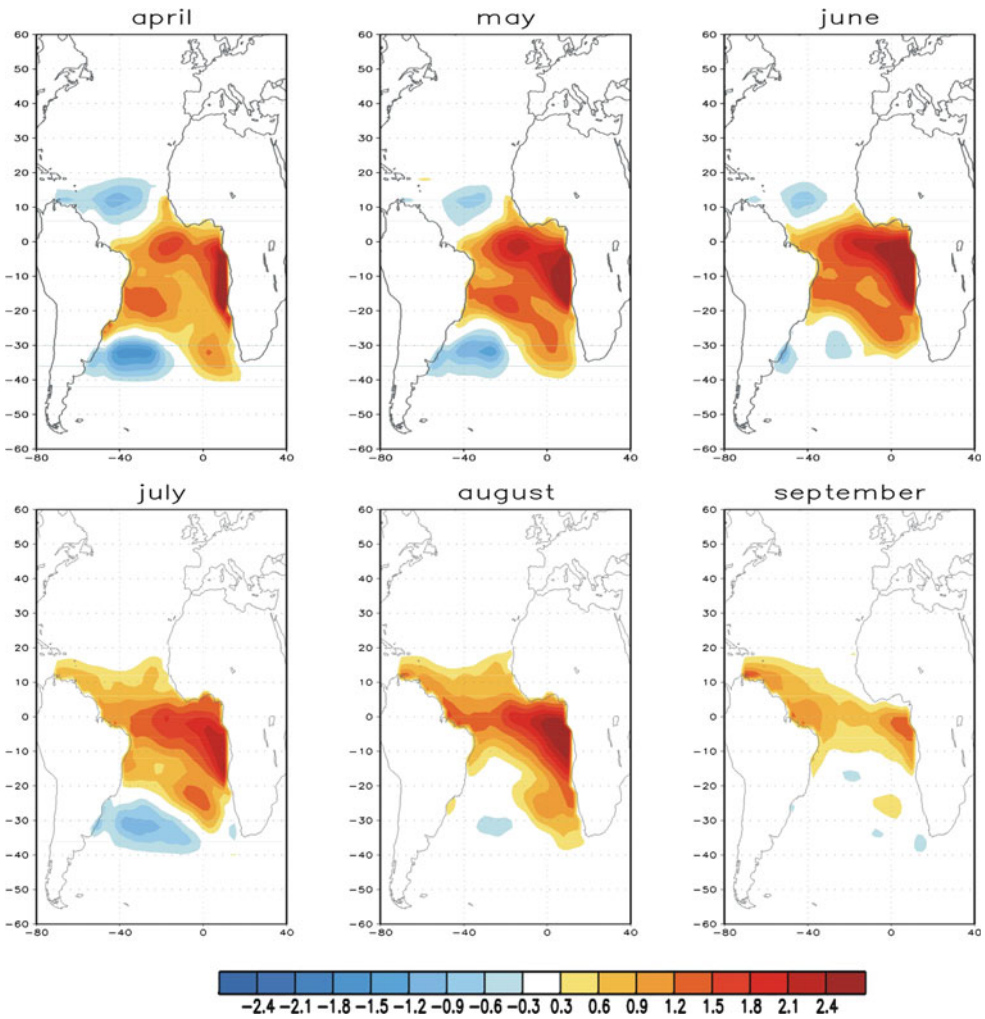

Fig. 1 April–September anomalous SSTs (°C) used as boundary conditions for EMP

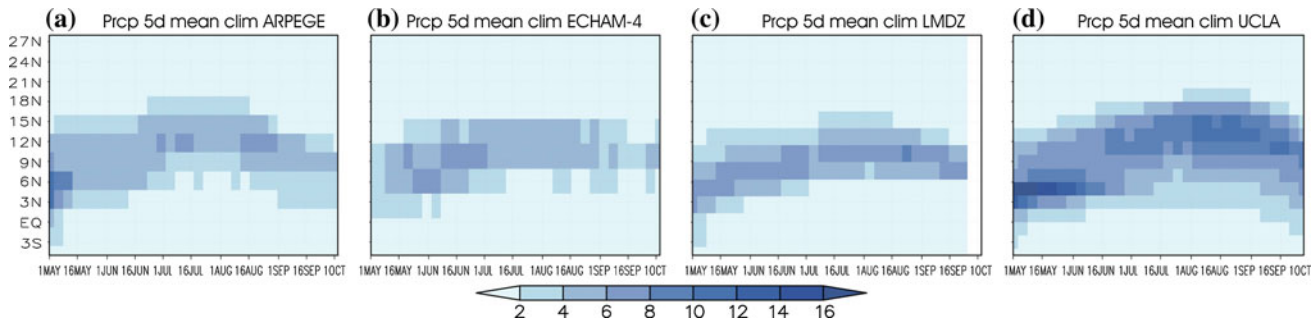

Fig. 2 5-day mean latitude by time precipitation (mm day^{-1}) from May to October, averaged over 10°W–10°E for (**a**) ARPEGE, (**b**) ECHAM-4, (**c**) LMDZ, (**d**) UCLA climatology

UCLA model has a good representation of the situation and amplitude of the heat low in summer. ARPEGE and ECHAM-4 present several minimums of pressure, while LMDZ and UCLA heat low are more zonally elongated. All the models properly simulate the southwesterly monsoonal wind although the amplitude of the monsoon winds is only realistic for ARPEGE. The circulation is too zonal in UCLA, which is consistent with the more zonally elongated heat low presented by this model. The monsoonal surface winds of ECHAM-4 and UCLA are much weaker than the observed. In the case of ECHAM this could be explained because the heat low amplitude is small in comparison with ERA-40 data, leading to a reduction of surface pressure gradient in this model. Also, the strong

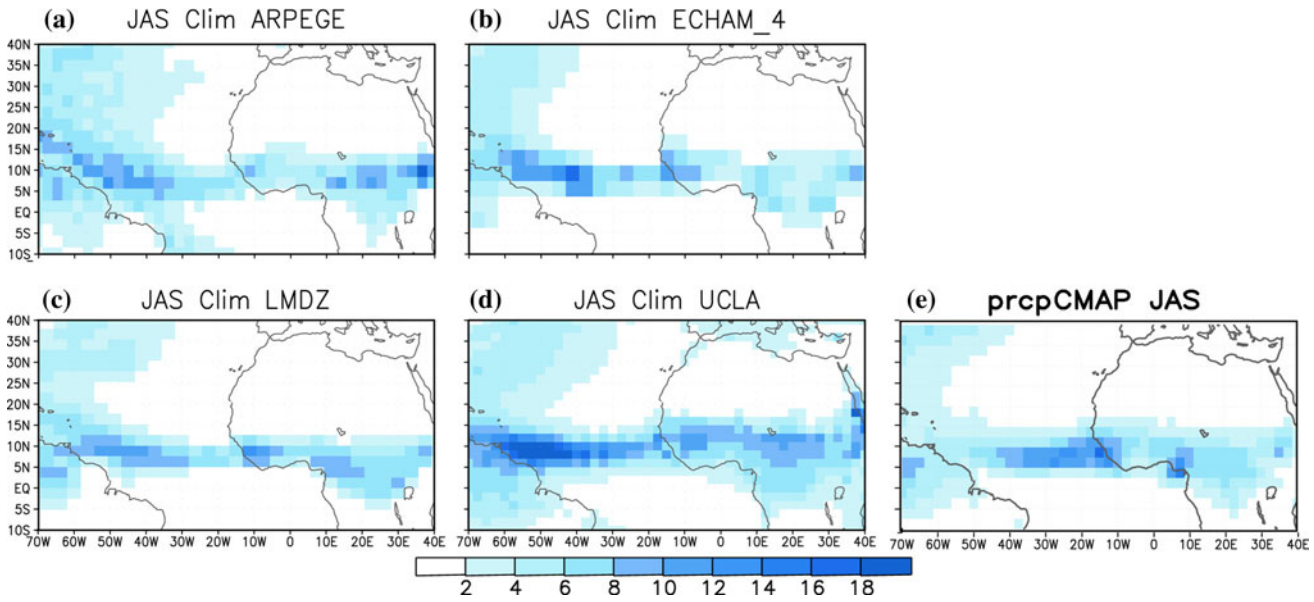

Fig. 3 JAS mean precipitation (mm day^{-1}) for (**a**) ARPEGE, (**b**) ECHAM-4, (**c**) LMDZ, (**d**) UCLA climatology and (**e**) CMAP precipitation averaged for the period 1979–2002

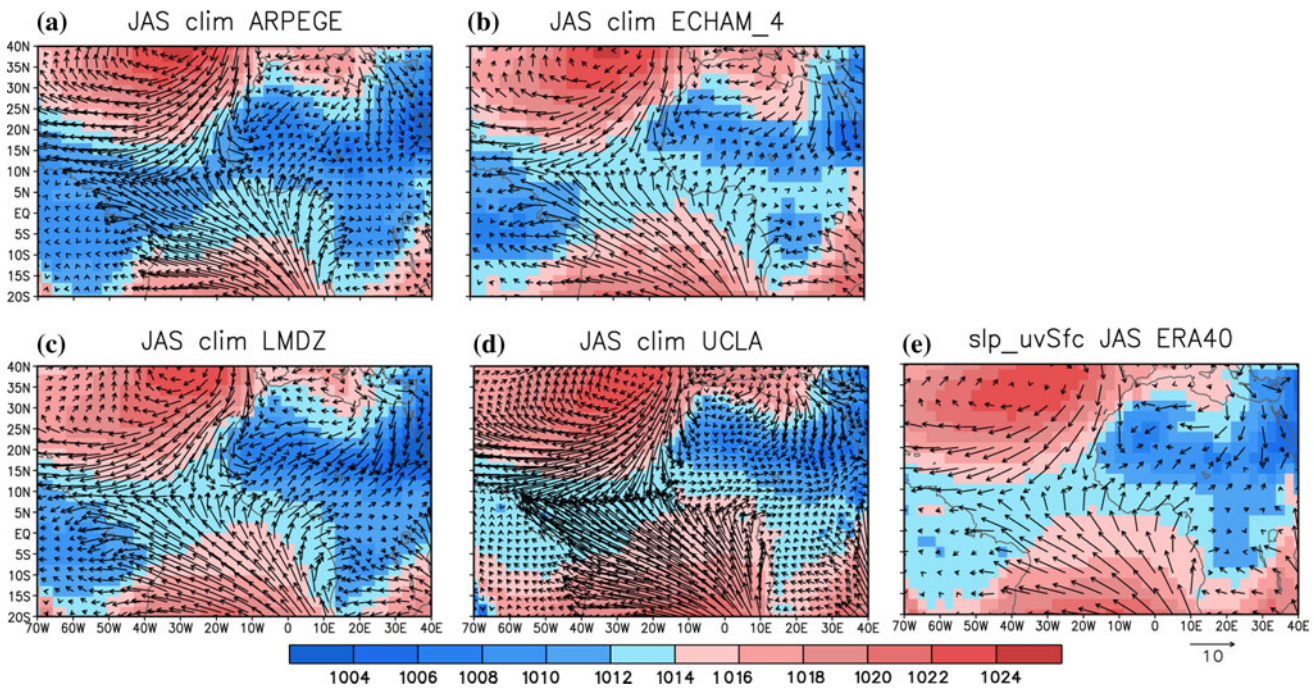

Fig. 4 JAS mean sea level pressure (MSLP; shaded; hPa) and surface winds (*arrows*; m s^{-1}) for (**a**) ARPEGE, (**b**) ECHAM-4, (**c**) LMDZ, (**d**) UCLA climatology and (**e**) ERA40 data averaged for the period 1979–2002

surface wind convergence over sea at 10°N in all the models, stronger in UCLA and ARPEGE, could be altering the course of the monsoon flow. Sultan and Janicot (2003) proposed a mechanism for the northward shift of the rainbelt, associated with the amplification of the heat low, in which the relative high pressure located to the north of the Atlas mountains would have a relative low associated to the south that will enhanced the Saharan heat low. This reinforcement would strengthen the northern branch of the Hadley cell, leading to a positive feedback that would end in the shift of the african rainbelt. The summer climatology of all the models present the relative high associated with

the Atlas and the westerly flow from the tropical Atlantic related to the relative low at the south of the mountains, thus representing fair well the effect of the orography in the West African atmospheric circulation. This feature is too zonal in UCLA model, which could explain the northward displacement of the rainfall belt observed in this model.

The inter-hemispheric pressure gradient between the heat low and the South Atlantic also plays an important role, as it leads to a region of inertial instability that produces an off-equatorial convection and a surface westerly jet (Tomas and Webster 1997).

The monsoonal circulation of the four models is also depicted in Fig. 5, where the cross-sections of the zonal, meridional and vertical winds averaged between 10°W and 10°E are plotted. The vertical circulation associated with the monsoon surface circulation (rising motion over 10°N and sinking motion to the equator) is well simulated by the models. ECHAM-4 upward motions associated with the deep convection are smaller in amplitude than the observed ones. The models simulation of the dry convection (around 20°N) is also in agreement with the observations. UCLA and, in a weaker way, LDMZ show a subsiding motion in the lower troposphere, between deep and dry convections, that is very weak in the observations.

In the middle and upper troposphere, north of the monsoon circulation, there is the northern local Hadley-type circulation already described by Vizy and Cook (2002). This circulation is present in all the models although UCLA is the most realistic one. Just below this circulation, the upward motions associated with the Saharan heat low appear for all the models. This upward motion reaches the middle troposphere, where the subsidence of the local Hadley limits the ascendance, and the air is then directed to the equator.

The tropical easterly jet (TEJ) at the top of the troposphere and the African easterly jet (AEJ) in the middle troposphere divert part of the monsoonal flow to the west (Vizy and Cook 2002). Both jets have been proved to be very important in WAM development (Gu and Adler 2004). The location of the jets is well simulated by the models, being the AEJ placed around 15°N at 600 hPa, and the TEJ at 9°N and 200 hPa, except the ECHAM-4 TEJ that is located too high and too far north and is very weak. LMDZ TEJ and ARPEGE AEJ are also too weak compared with ERA-40. The amplitude of UCLA jets is in more agreement with the observations, although the TEJ is a bit stronger than the observed one.

The monsoonal surface westerly flow is present in all the models, being too strong for UCLA and too weak for ECHAM-4. It is worth to notice that the climatological circulation of ECHAM-4 clearly resembles the structure depicted by Nicholson (2009) and Nicholson and Webster (2007) for dry Sahelian years. This is consistent with the weak wet convection and TEJ that this model present.

Overall, despite of the differences between models pointed above, the main characteristics of the WAM are reasonably well reproduced by the four models, proving them to be a useful tool in the study of the WAM dynamics.

3.2 Models response to Equatorial Mode

In this section we try to understand the impact of the Equatorial mode in this seasonal evolution of the African monsoon.

Figure 6 represents the latitudinal seasonal evolution of the 5-day mean rainfall averaged over the region 10°W–10°E, for the EMP and EMN experiments and for all the models. For the positive cases, all the models show a clear distinction in the location of the maximum rainfall between May and June (MJ) and JAS. During MJ, the maximum rainfall is located in the equatorial belt, around 5°N while in JAS, this maximum is displaced north, up to 12°N. ECHAM4 and LMDZ give the JAS maximum south of the UCLA and ARPEGE one, being also weaker in amplitude for the former models. This clear distinction in the precipitation behavior has let us continue the analysis focusing in the description of MJ and JAS means. It is clear how, for all the models, the precipitation in EMP is higher than normal in the GG region during MJ, while the opposite occurs in EMN simulation. The difference in the onset date between EMP and EMN is also very apparent: the onset date is delayed in EMP, while it appears earlier in EMN. This feature is clearer for UCLA, but is present in all the models. From Fig. 6 is also noticeable that the migration of the rainbelt goes further north in EMN than in EMP. Figure 7 depicts the horizontal anomalous rainfall maps for the MJ and JAS selected periods and the positive experiment. There can be seen marked dipolar features between the anomalous rainfall north and south of 5°N during MJ, although ARPEGE does not give this for the African region. For JAS, the dipolarity persists although weaker for all the models, the anomalous positive rainfall belt is displaced north and the precipitation is weakened north of 10°N, although less intense for UCLA and ARPEGE simulations. LMDZ response is shifted to the south with respect to the rest of the models, presenting negative precipitation anomalies from 8°N.

In order to study this dipolar behaviour in the precipitation anomalies for all the models and the positive and negative experiments, we have computed two indexes of anomalous precipitation over the Sahelian and the Guinean regions for all the models and simulations. These were calculated by computing the mean precipitation between 10°W and 10°E and 11–18°N for the Sahelian

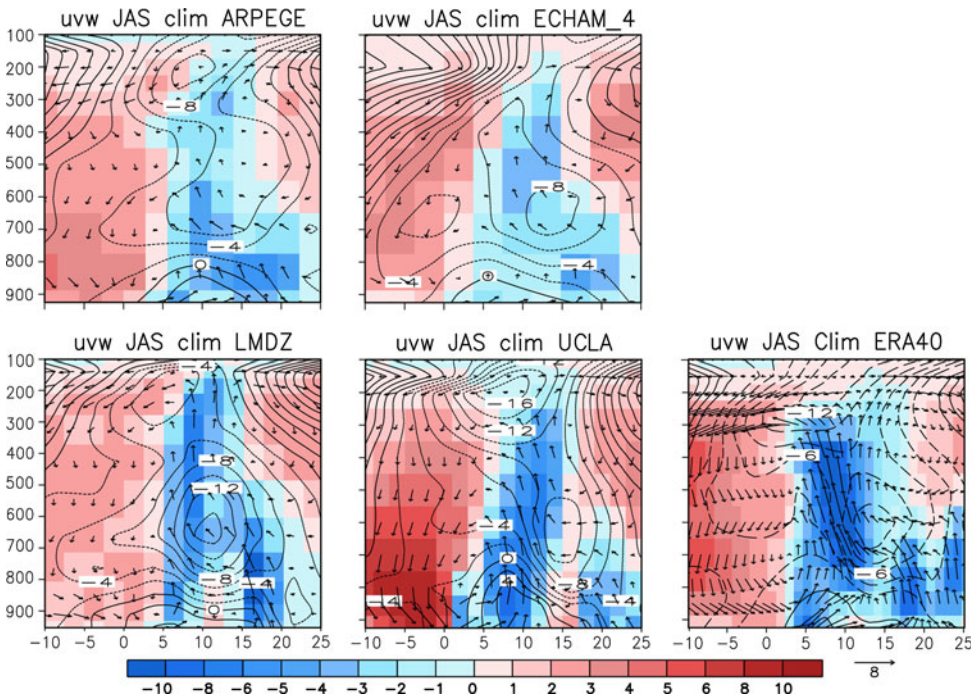

Fig. 5 Same as Fig. 4 but for 10°W–10°E averaged vertical velocity (*shaded*; 100 × Pa s^{-1}), zonal wind (*contours*; m s^{-1}), and omega-meridional wind (*arrows*; m s^{-1}, 100 × Pa s^{-1})

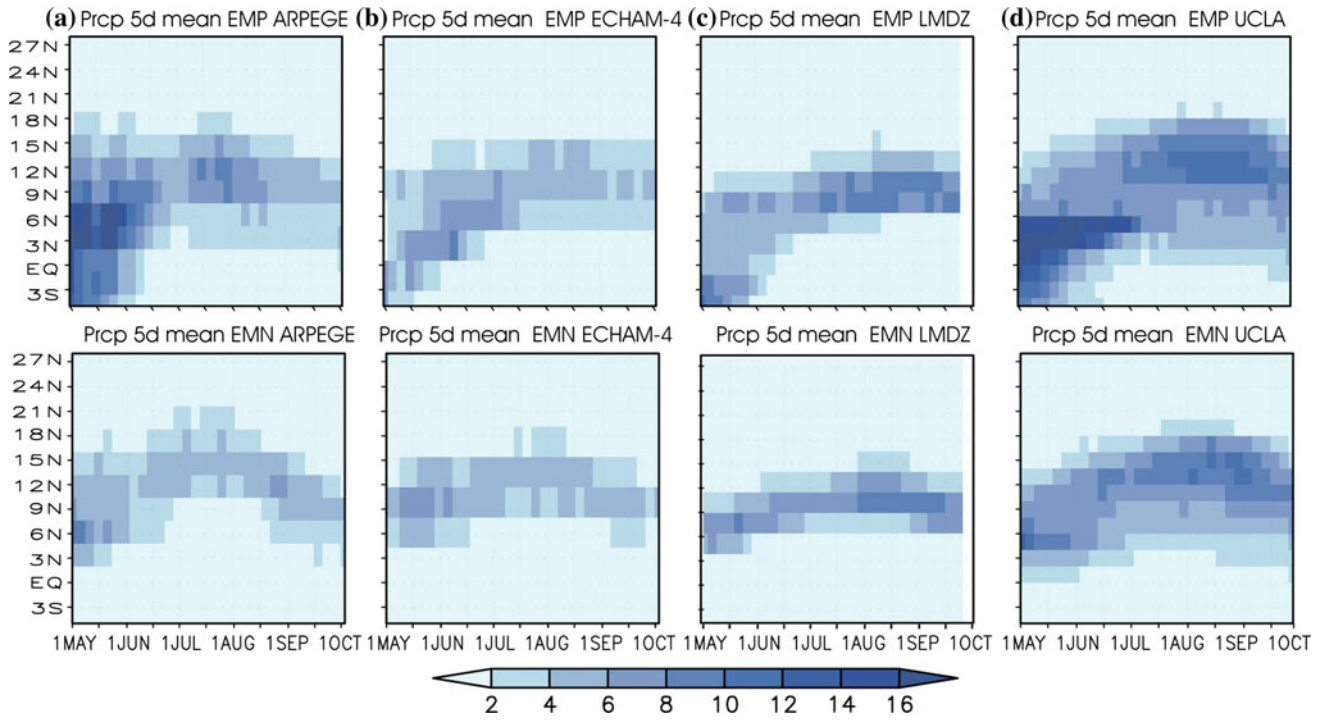

Fig. 6 5-day mean latitude by time precipitation (mm day^{-1}) from May to October, averaged over 10°W–10°E for EMP (*top*) and EMN (*bottom*) and for (**a**) ARPEGE, (**b**) ECHAM-4, (**c**) LMDZ, (**d**) UCLA

index, and 10°W–10°E and 0°–8°N for the Guinean one, for the climatology and for each of the members of the ensembles EMP and EMN. Then, we have calculated the anomalous value for each member of the ensembles by subtracting the climatological value from the control simulation. Figure 8 shows the values of the indexes for all the models. All the EMP simulations present positive anomalies over Guinea except one member of ECHAM-4. For the Sahelian region the results are negative for almost all the simulations. UCLA and LMDZ show small

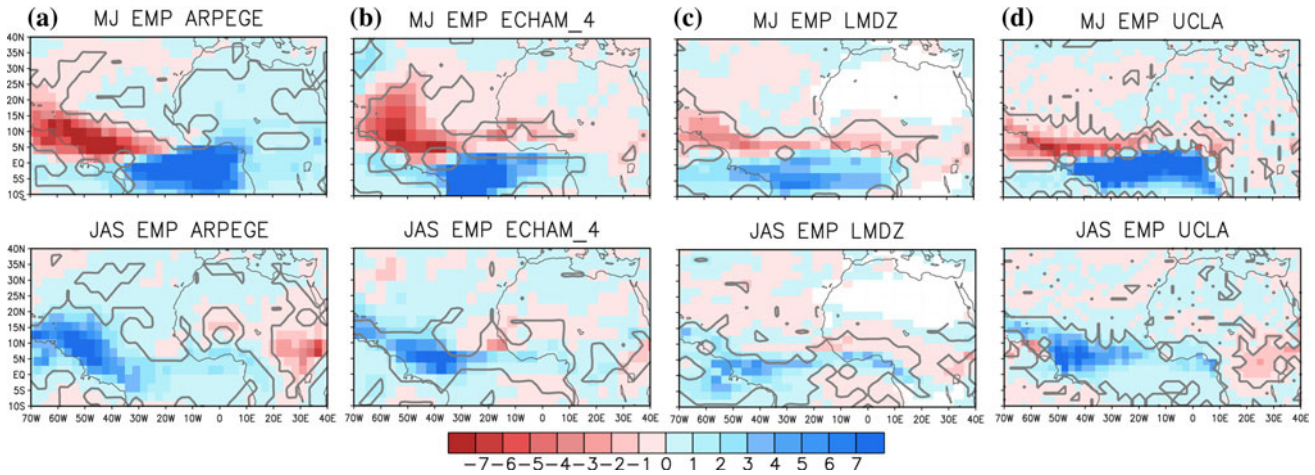

Fig. 7 Anomalous precipitation (mm day^{-1}) for (**a**) ARPEGE, (**b**) ECHAM-4, (**c**) LMDZ and (**d**) UCLA EMP simulation for May–June (*top*) and July–September (*bottom*). *Grey line* delimits the areas in which precipitation values exceed the 95% significance level

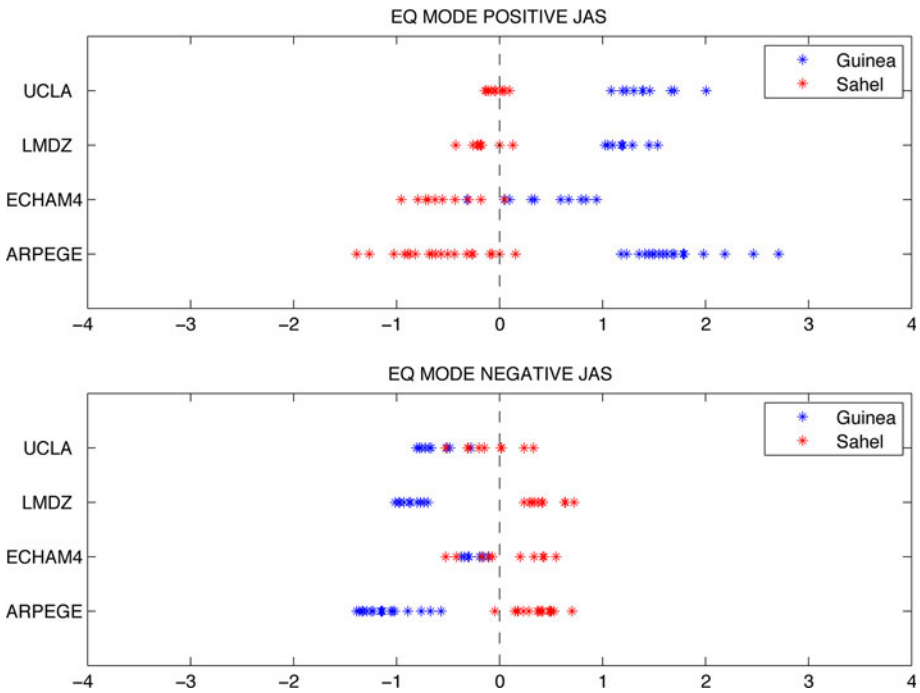

Fig. 8 JAS averaged anomalous precipitation (mm day^{-1}) for Guinean (10°W–10°E, 0°–8°N) and Sahelian (10°W–10°E, 11–18°N) region, computed for each model and each member of the EMP and EMN simulation

dispersion of the anomalies, while ECHAM-4 and ARPEGE dispersion is higher. In general the magnitude of anomalies is smaller for the Sahelian region. The results of the EMN simulation over GG are opposite to the EMP ones, but the anomalies are in general weaker and present a smaller dispersion. The dipolar structure of the anomalies in EMN is clear for LMDZ and ARPEGE; ECHAM-4 shows this structure in 5 of the 10 members of the simulation, and UCLA in just 2 of the 10 members. Thus, the Sahelian precipitation response to a negative anomaly of SST over the Gulf of Guinea is weaker and less consistent than the response to a positive anomaly. Although the response is weaker in EMN than EMP and, thus, non-linear, Fig. 8 point to the robustness and importance of the linear part of the response. For the sake of simplicity, from now we will focus on the linear part of the response, and we will only show results from EMP simulations. Additional work is needed for the analysis of the non-linearities, buy this is out of the scope of this paper and will be achieved in future works.

In order to study the dynamical features involved in the seasonal anomalous response to the Equatorial SST mode,

first, we will analyze the Saharan heat low response to this tropical Atlantic heating, taking into account that most of recent studies focus on the dynamics of the low as a crucial factor determining the monsoon onset, either by itself (Sultan and Janicot 2003; Ramel et al. 2006; Hagos and Cook 2007) or as part of the inter-hemispheric pressure gradient (Nicholson 2009; Nicholson and Webster 2007). Figure 9 depicts the MJ and JAS MSLP and surface wind anomalies for the four models. All the models show surface wind convergence over the regions of the maximum anomalous SSTs (see Fig. 1), and associated low-pressure anomalies, together with warm air temperature anomalies (not shown). During MJ, the low pressure anomalous centre over the GG weakens the pressure gradient between GG and Saharan heat low, which is also noticeable in the surface wind anomalies with a weakening of the monsoonal circulation for all the models. During JAS, the anomalous convergence of winds is displaced westward and northward than in MJ, and there is a diminishing of the MSLP over the whole basin. The moisture convergence zone appears displaced to the south in EMP (not shown), with a maximum convergence anomaly that moves from the equator (MJ) to 10°N (JAS) in all the models. North of this convergence, all the models show a weak anomalous moisture divergence, consistent with a decrease of precipitation in that area.

The latitude by height anomalous circulation averaged between 10°W and 10°E is plotted in Fig. 10. The northward migration, from May to August, of the deep convection appears in all the models (see arrows in Fig. 10). In this way, before the onset (MJ) and due to the underneath heating, the deep vertical movements associated with the deep convection are reinforced and shifted to the equator in all the EMP simulations. Also due to the underlying SST anomalies, after the onset (JAS), EMP deep convection is still located a bit to the south than for CONTROL (Fig. 5), but it is stronger in magnitude.

Although the position of the dry convection is similar in EMP and CONTROL for all the models (not shown), it is weak for MJ and JAS, as it can be seen in the anomalous downward flow in the region of the Sahara heat low; this feature is really clear for ARPEGE, UCLA and LMDZ, though for the latter it is shifted to the south (in agreement with the smaller northward migration of the rainfall belt present in this model). For ECHAM-4 the anomalous subsidence is weaker and located in the northward flank of the dry convection. Also, the upper tropospheric subsiding motions are also reinforced and shifted to the south, showing downward anomalies around 15–20°N in all the models. The position of this anomalous downward movements differ from one model to another, being located further south for LMDZ (anomalous subsidence is located around 10–12°N and 300 hPa for this model, while it is placed at 15°N for ECHAM-4, and cover the whole Saharan region for ARPEGE and UCLA).

In relation to the zonal anomalous winds (contours in Fig. 10), most of the models (clearer in ARPEGE and UCLA) show, south of 7°N, from lower levels and up to the middle troposphere, a change between westerlies in MJ to easterlies in JAS. This change in the surface winds is also present in Fig. 9, as a result of the change in the location of the anomalous surface convergence- over the anomalous positive SSTs- between MJ and JAS. Also, north of 7°N, anomalous easterlies are reinforced from MJ to JAS in all the models.

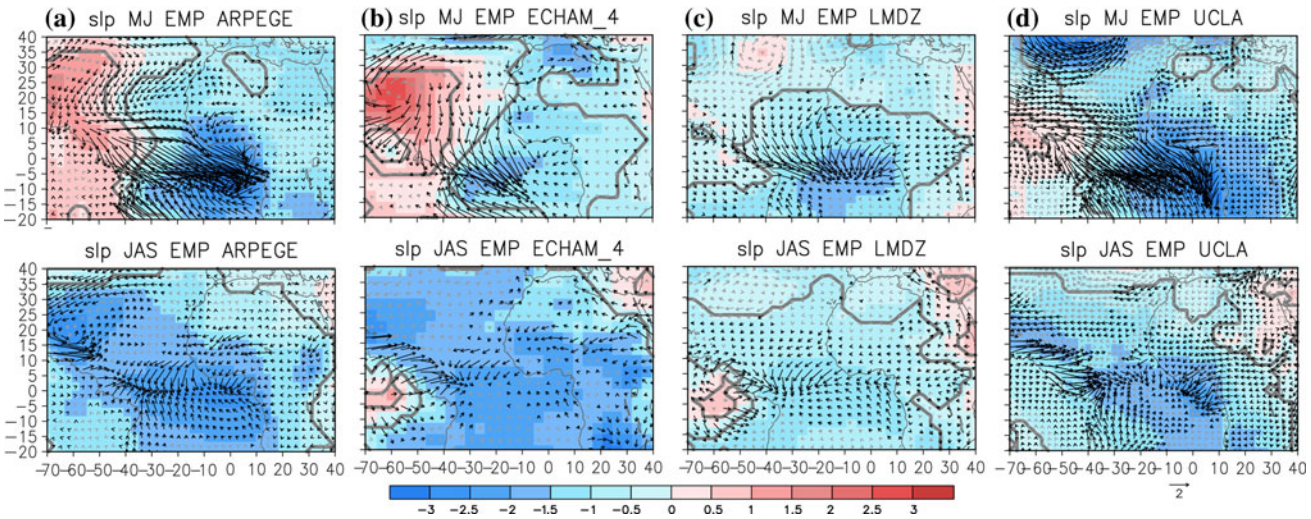

Fig. 9 Anomalous MSLP (*shaded*; hPa) and surface winds (*arrows*; m s^{-1}) for (**a**) ARPEGE, (**b**) ECHAM-4, (**c**) LMDZ and (**d**) UCLA EMP simulation for May–June (*top*) and July–September (*bottom*). *Grey line* delimits the areas in which MSLP values exceed the 95% significance level. *Black arrows* correspond to surface wind anomalies that exceed the 95% significance level

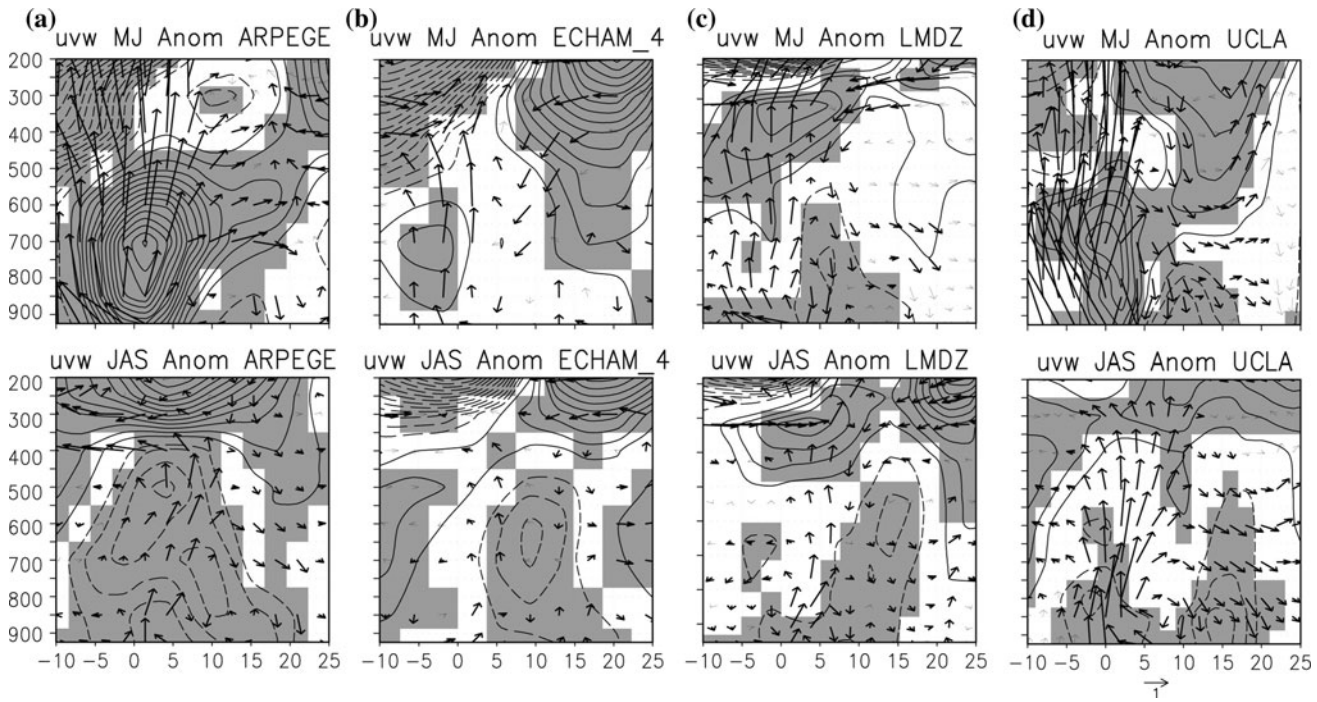

Fig. 10 Same as Fig. 7 but for 10°W–10°E averaged zonal wind (*shaded*; m s^{-1}), and omega-meridional wind (*arrows*; m s^{-1}, 100 × Pa s^{-1}). *Shaded regions* denote those areas where the zonal wind anomalies exceed the 95% significance level

The AEJ appears reinforced in JAS for all the models, although weaker for UCLA. In the upper troposphere, the zonal wind shows a weakened TEJ for all the models, a feature that has been reported to be coherent with the reinforcement of the AEJ (Nicholson and Grist 2003). We exclude ECHAM-4 of this discussion, as we do not find a good performance of the TEJ in this model (see Fig. 5).

The upper level zonal wind presents anomalous easterly flow to the south of the maximum anomalous upward motions, and anomalous westerlies to the north. This anomalous cyclonic circulation can be associated with a Gill response to the tropical heating (Gill 1980). Even though the location of this cell varies from one model to another, it is present in all the models for MJ. During JAS, this feature is very clear in ECHAM-4 and LMDZ, while it is very weak for UCLA and does not appear in ARPEGE. Looking at the 200 hPa anomalous streamfunction (not shown), we find that in JAS the anomalous cyclonic anomaly is more shifted to the west in ARPEGE and UCLA than in ECHAM-4 and LMDZ, explaining the differences between models in the 200 hPa zonal circulation.

As it was already mentioned, the four models show a dipole of precipitation between GG and Sahel. Wet conditions over the Gulf of Guinea and GG coast and dry ones around 15°N are easily explained as a response to the anomalous ascending motions over GG, and the weakening of the surface convergence over the Saharan heat low (see Fig. 9).

The situation is rather different when we focus on the Sudan-Sahel region (between 7 and 12°N). In order to explain the precipitation anomalies in this area, we focus on the vertical circulation in the lower and middle troposphere over these latitudes.

The behaviour of the middle and lower atmosphere is opposite: precipitation anomalies are positive around 7–9°N, where anomalous subsidence is present in the lower troposphere and anomalous upward motions appear in the middle troposphere; the opposite occurs around 10–12°N, in a region where anomalous upward motions appear near the surface for all the models but UCLA, anomalous subsidence being present in the middle troposphere together with dry conditions. Thus, we cannot explain the precipitation behaviour over this area as a response to the low level circulation. The dipolar behaviour in the precipitation anomalies in EMP could in turn be explained as a response to the large-scale dynamics associated with the southward displacement of the monsoonal circulation produced by the weakening of the MSLP gradient. The reinforcement and the southward displacement of deep convection would lead to an anomalous downward circulation in the middle-upper troposphere. In this way, we find positive precipitation anomalies in 7–9°N (Fig. 7) coinciding with anomalous upward motions in the middle troposphere (Fig. 10), and the opposite to the north (negative precipitation anomalies in 10–12°N together with downward motions in the middle troposphere). These subsiding motions, together with the

weakening in the Saharan convergence would produce a decrease of the precipitation north of 10°N. The inhibition of the westerly flow from the subtropical Atlantic Ocean around 15–20°N (in all the models after the onset, see Fig. 4), can also contribute to the Sahelian drought, by bringing less moisture into the zone.

The lower troposphere upward motions in 10–12°N (present in all the models but UCLA) and downward at 7–9°N could, in turn, be a response to the precipitation field instead of a cause of it. In this way, the decrease (increase) of precipitation around 12°N (7–9°N) would lead to an increase (decrease) of the surface sensible heat flux to the atmosphere in the region (not shown), this would warm (cool) the lower atmosphere producing superficial ascending (descending) motions locally. The sensible heat flux anomalies in UCLA are very small, which could explain the absence of the local upward motions in this model.

Thus, our results differ from those of Vizy and Cook (2002) that explained the precipitation dipole as a local response over the southern Sahel to low level downward motions associated with the weakening in the Saharan convergence.

The location and strength of the AEJ has been reported to be key features determining the West African precipitation (Cook 1999; Gu and Adler 2004). We now focus on the characteristics of this jet in the EMP simulations, trying to understand the way in which it can influence the precipitation.

There are several differences regarding the simulation of the AEJ by each of the models. For the CONTROL, ARPEGE AEJ is too weak until September, when it is placed around 700 hPa (Fig. 5). For the EMP simulation, the ARPEGE AEJ is well defined during the monsoon season (JAS), and a local maximum of negative zonal wind is already located at 700 hPa in July. ARPEGE and UCLA show, as a response to the Equatorial mode, a decrease in the magnitude of the AEJ before the onset, followed by an increase after that. LMDZ and ECHAM-4 present a reinforced AEJ already in MJ, although it is not significant for ECHAM-4 (Fig. 10).

As it has been documented by other authors, the strength and position of the AEJ is controlled by the surface temperature and moisture gradients and the vertical shear (Cook 1999; Sultan and Janicot 2003; Nicholson and Grist 2003). Here we analyze the relationship between precipitation, surface temperature and AEJ model by model, in order to explain the evolution of the AEJ during the monsoon season (Fig. 11). For ARPEGE model, during May and June, AEJ maximum is located around 12°N in EMP simulation. Precipitation anomalies are positive for almost all West Africa, with the exception of a small negative anomaly over Senegal. The surface temperature anomaly presents a dipole with negative anomalies over Sahara and positive anomalies south of 10–15°N (not shown). This anomalous pattern of surface temperature produces a negative gradient of surface temperature at the jet latitudes (Fig. 11), causing the jet to decrease. During JAS precipitation anomalies are negative north and below the AEJ (still located at 12°N), and positive to the south. Surface temperature anomalies are positive over Sahel and

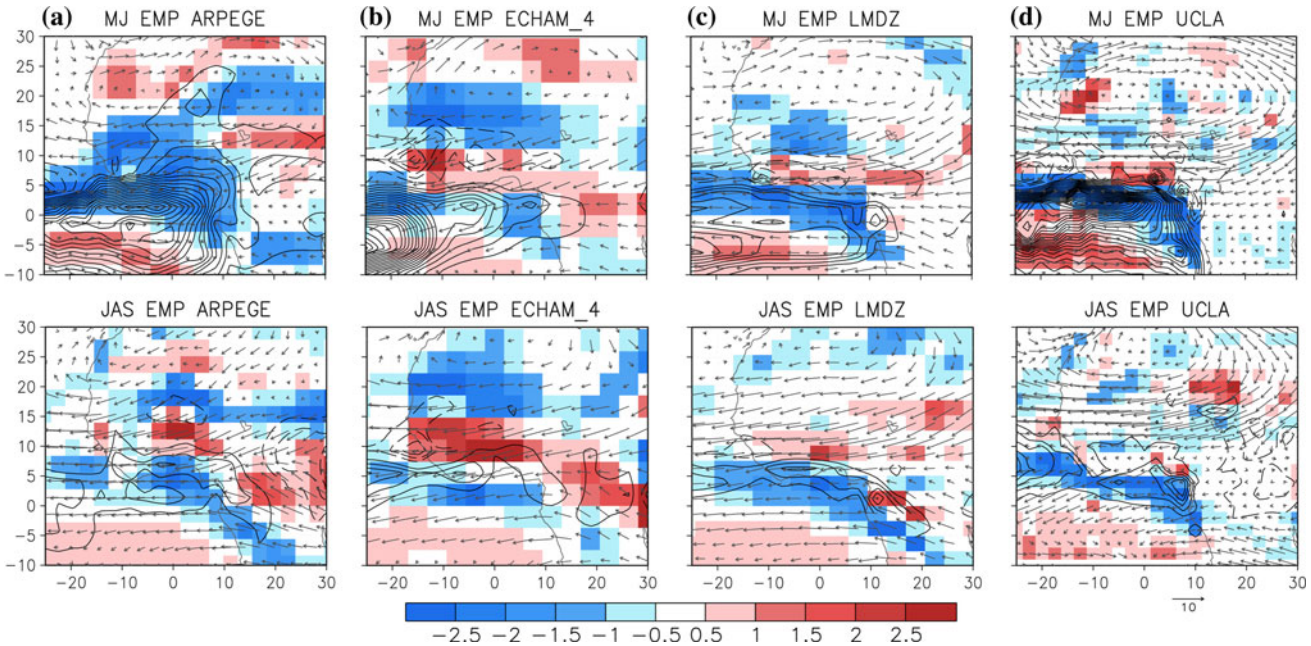

Fig. 11 Same as Fig. 7 but for anomalous precipitation (mm day^{-1}), and surface temperature gradient (10^6 × °C m^{-1}), together with mean JAS 700 hPa zonal wind (m s^{-1})

Guinea coast; its maximum anomaly is located always north of the latitude of the jet, which implies a negative gradient of surface temperature to the north and a positive gradient at the jet location, thus producing a reinforcement of the AEJ during the monsoon season.

ECHAM-4 AEJ response is weak during MJ. During this season, the jet is located at 9°N, in a region of negative precipitation anomalies, the maximum of this precipitation anomalies is located to the north of the maximum AEJ, producing negative temperature gradient to the north and positive one to the south, just below the AEJ, leading to a slight (not even significant) reinforcement of it. In JAS, the situation is similar, and the AEJ is located around 14°N, over a region of positive temperature gradient that would cause the jet to increase.

For LMDZ we find that in EMP the jet is strengthened during the whole period of study. Its maximum is located at 8°N in MJ, and around 11°N in JAS. In every month the jet is located above a region of negative precipitation anomalies and positive surface temperature anomalies with its maximum displaced to the north with respect to the jet location; the surface temperature gradient will decrease to the north and increase to the south of the maximum surface temperature anomalies, leading to a reinforcement of the jet during the whole period.

Regarding UCLA EMP results, during MJ precipitation is weakened below the jet (12°N), with a minimum to the south. Surface temperature increases; showing its maximum anomaly south of the jet, the temperature gradient decrease over the jet and it weakens. During JAS the precipitation anomalies are again negative, but now the maximum of the anomalies is located north of the jet latitude (15°N), the maximum surface temperature anomaly is then placed to the north of the jet, and the surface temperature gradient at the jet location increases, strengthening the AEJ. For this model, the pattern of anomalous temperature gradient is very noisy, and as a consequence, the response of the AEJ is weaker.

From our results, the changes in precipitation over the Sahel, resulting from the Equatorial mode, seem to be controlling the intraseasonal variability of the AEJ. Nicholson and Grist (2003) reported the possibility of the precipitation influencing the AEJ. Our results confirm this and point to an influence of the Atlantic equatorial SST on the AEJ, through the impact of precipitation anomalies in the development of the jet. If precipitation decreases over the Sahelian area, the soil moisture content and evapo-transpiration will also decrease; if less moisture is available, the heat fluxes will be balanced by increasing the sensible latent heat flux to the atmosphere, causing the surface air temperature to increase. This will affect the local surface temperature gradient, which will be stronger to the south of the maximum air temperature anomaly, and weaker to the north. UCLA AGCM shows the weakest response in terms of surface heat fluxes. It is worth to notice that this model does not have an interactive soil moisture content, which could lead to a less realistic fluxes, thus explaining the noisy response. Cook (1999) results point that the jet features are determined by the characteristics of the strong surface temperature gradient located at the latitude of the jet. Our results agree with them, as we find that the reinforcement or weakening of the jet is strongly related with the magnitude and position of the precipitation anomalies, which control the local surface temperature gradient anomalies, in all the models of the study. Several studies point to the AEJ influence on Sahelian precipitation (Lare and Nicholson 1994; Cook 1999; Nicholson and Grist 2003; Gu and Adler 2004), a strong AEJ would inhibit moisture convergence north of the jet leading to a positive feedback between precipitation and AEJ anomalies.

Even though there are important differences between models, mostly related to the differences regarding the land-atmosphere feedbacks, in the WAM region, the responses to a positive anomaly in the equatorial Atlantic Ocean are consistent and can be summarized as follows: The warming of the tropical Atlantic weakens the sea-land temperature and pressure gradient that drives the monsoonal circulation. Due to the equatorial anomalous heating, the monsoon circulation is shifted to the south, the ascending motions over the Guinean coast and the Gulf of Guinea are strengthened and precipitation increases over this area. At the same time, the subsiding motions in the middle and upper troposphere are enhanced further north, just above the region where the surface convergence between the monsoon flow and the Saharan northeasterly flow weakens, so do the upward motions related to it. This situation leads to a dipole of anomalous precipitation, determined by the large scale related to the anomalous SST pattern. Locally, the anomalous precipitation pattern, in turn, affects the surface heat fluxes, and this produces local changes in the low level circulation and the temperature gradient at the latitude of the AEJ, leading to an increase in its strength. A positive feedback between AEJ and precipitation anomalies would produce an increase in the anomalies through the monsoon season, until the seasonal cycle restores the mean circulation after the monsoon season.

4 Summary and conclusions

In this study, we first analyzed the skill of four AGCM (ARPEGE, ECHAM-4, LMDZ, UCLA) in simulating the West African Monsoon dynamics, during the last decades of the XXth century. Then, we focus on the impact of the

Atlantic Equatorial mode on the West African Monsoon for the same period of study.

The simulation of the annual evolution of the precipitation is consistent for all the models, which place the onset at the end of June, in concordance with the observations (Sultan and Janicot 2003). All the summer precipitation patterns are consistent with the observed one, although there are some differences between models: UCLA model rainbelt goes too far north, and its magnitude and width are stronger than the observed one; on the contrary, LMDZ shows a precipitation pattern narrower than the observed, with a weak northward shift of the african rainbelt.

The main characteristics of the heat low and its interaction with the orography are also well simulated for all the models. In our simulations, the model that shows a southward displacement of the heat low (LMDZ) also presents the located too far south with respect to the observations; conversely, the model with the heat low situated more to the north (UCLA) is the one that shows the summer rainbelt more shifted to the north. Also, the models that show a zonally elongated heat low (UCLA, LMDZ) show a more zonal monsoonal circulation. Thus, the results support the idea that the location of the heat low seems to be a key factor in the monsoonal circulation and in the abrupt shift of the rainbelt (Hagos and Cook 2007; Ramel et al. 2006; Sultan and Janicot 2003). The results are also compatible with the perspective of the heat low as a part of an inter-hemispheric pressure gradient that drives dynamic instability over the monsoon area (Nicholson 2009; Nicholson and Webster 2007).

Despite of the differences between models, the deep and dry convections are also well simulated by all of them, so are the African and Tropical Easterly Jets; with the exception of ECHAM-4 TEJ, that is too weak and located too north and too high in the troposphere. Overall, the results prove that all the models have a good simulation of the WAM climatology, and can be used for the study of the WAM and its interactions with different SST patterns.

The influence of the Equatorial mode on the WAM has been studied by analysing four ensemble simulations (each one performed with each AGCM), in which the Equatorial mode anomalies have been added to the 1979–2005 climatological SSTs. The boundary conditions have been designed resembling the leading time-varying Tropical Atlantic SST mode that maximizes the covariance with the summer WAM rainfall (Polo et al. 2008) from the period 1979–2003; and which corresponds to the Equatorial mode. Results are robust and similar in the four models, despite of the differences between them. They show a dipole of anomalous precipitation in all the models and for almost all the members of the ensembles, with positive (negative) precipitation anomalies over the GG (Sahel) region and negative ones over the Sahel (GG) for warm (cold) SST anomalies over the equatorial Atlantic. The response is stronger for the warm SST simulations than for the cold SST one, pointing to the presence of non-linearities; for the sake of simplicity, this paper has focused in the linear part of the WAM response to the Atlantic equatorial SST anomalies, in a future work, additional analysis will be done in order to study the non-linear part of the response.

The main atmospheric response to a warming in the equatorial Atlantic during summer is the diminishing of the mean sea level pressure gradient between the equator and the Saharan heat low. This causes the weakening of the monsoonal circulation, shifting it to the south. The northward displacement of the rainfall belt is less pronounced and wet convection is located further south than its climatological position, leading to an increase of the precipitation south of approximately 10°N, depending on the model. For all the simulations, the latitude where the upward motion in the middle troposphere turns downward is the northern limit of the positive precipitation anomalies. North of this point, as a response to the reinforcement of the convection, there are strong anomalous subsiding motions in the middle and upper troposphere for all the models, together with anomalous dry conditions. These results point to the large-scale dynamics and the modulation of the upper level Hadley-type circulation, related with the anomalous SST, as the responsible of the anomalous precipitation dipole.

Our results then differ from those of Vizy and Cook (2002), that relate the anomalous negative precipitation over the southern Sahel with the low level subsiding motions over the area. On the contrary, three of our models (all except UCLA) show anomalous low level downward motions over the northern part of the region of positive precipitation anomalies, and all of them present anomalous low level upward motions to the north, in the southern region of the negative precipitation anomalies. The local response to the anomalous precipitation pattern modifies the surface fluxes along West Africa, a decrease (increase) of the precipitation causes a decrease (increase) of the latent heat flux and a increase (decrease) of the sensible heat flux to the atmosphere, leading to a warming (cooling) of the surface and to the local upward (downward) motions.

The modification of the surface fluxes also influence the surface temperature gradient at the latitude of the AEJ, causing it to increase after the onset in all the models. In this way, as the AEJ favors the moisture convergence to the south and inhibits it to the north (Nicholson and Grist 2003), we find a positive feedback between precipitation and the AEJ through all the monsoon season. The reinforcement of the AEJ is clear for all the models, being UCLA the one that shows a weaker response.

The main differences between UCLA and the rest of the models are found in the processes in which the surface

fluxes are important. ARPEGE, ECHAM-4 and LMDZ have an interactive scheme of the soil wetness, while UCLA model has the soil wetness set to climatological conditions. If there is a decrease of precipitation in a model with interactive soil wetness, the amount of water available will decrease, and so will the evaporation. In order to balance the heat fluxes, the sensible heat to the atmosphere has to increase, leading to a warming of the surface. If the model doesn't have this interactive soil moisture, the total amount of available water will be constant, even if there is less precipitation, and the effect of the decrease of the precipitation on the surface fluxes will be underestimated. This would explain why the strengthening of the AEJ is very weak in the UCLA results, and also the absence of the local warming of the southern Sahel that appears in the rest of the models.

Acknowledgments This study was supported by the EU-AMMA project and the Spanish MEC project CGL2006-04471. Based on French initiative, AMMA was built by an international scientific group and is currently funded by a large number of agencies, especially from France, UK, US and Africa. It has been the beneficiary of a major financial contribution from the European Community's Sixth Framework Research Programme. Detailed information on scientific coordination and funding is available on the AMMA International website http://www.amma-international.org. The authors thank Javier García-Serrano and Elsa Mohino for his very useful comments on the manuscript, and the two anonymous reviewers for their constructive suggestions and comments.

References

Cane MA, Clement AC, Kaplan A, Kushnir Y, Pozdnyakov D, Seager R, Zebiak SE, Murtugudde R (1997) Twentieth-century sea surface temperature trends. Science 275:957–960. doi:10.1126/science.275.5302.957

Cook KH (1999) Generation of the African Easterly Jet and its role in determining West African precipitation. J Clim 12:1165–1184

Déqué M, Dreveton C, Braun A, Cariolle D (1994) The ARPEGE/IFS atmosphere model: a contribution to the French community climate modeling. Clim Dyn 10:249–266

García-Serrano J, Losada T, Polo I, Rodríguez-Fonseca B (2008) Tropical Atlantic Variability modes (1979–2002). Part II: time-evolving atmospheric circulation related to SST-forced tropical convection. J Clim 21:6476–6497. doi:10.1175/2008JCLI2191,1

Giannini A, Saravannan R, Chang P (2005) Dynamics of the boreal summer African monsoon in the NSIPP1 atmospheric model. Clim Dyn 25:517–535. doi:10.1007/s00382-005-0056

Gill AE (1980) Some simple solutions for the heat induced tropical circulation. Quart J Met Soc 106:447–462

Gu G, Adler RF (2004) Seasonal evolution and variability associated with the West African monsoon system. J Clim 17:3364–3377

Hagos SM, Cook KH (2007) Dynamics of the West African monsoon jump. J Clim 20:5264–5284

Hourdin F, Musat I, Bony S, Braconnot P, Codron F, Dufresne JL, Fairhead L, Filiberti MA, Friedlingstein P, Grandpeix JY, Krinner G, LeVan P, Li ZX, Lott F (2006) The LMDZ4 general circulation model: climate performance and sensitivity to parametrized physics with emphasis on tropical convection. Clim Dyn 27:787–813

Janicot S (1992) Spatiotemporal variability of West African rainfall. Part II: associated surface and airmass characteristics. J Clim 5:499–511

Janicot S, Harzallah A, Fontaine B, Moron V (1998) West African monsoon dynamics and eastern equatorial Atlantic and Pacific SST anomalies (1970–1988). J Clim 11:1874–1882

Janicot S, Trzaska S, Poccard I (2001) Summer Sahel-ENSO teleconnection and decadal time scale SST variations. Clim Dyn 18:303–320

Kucharski F, Bracco A, Yoo JH, Tompkins A, Feudale L, Ruti P, Dell'Aquila A (2009) A Gill-Matsun-type mechanism explains the tropical Atlantic influence on African and Indian monsoon rainfall. Quart J R Met Soc 135:569–579

Lare A, Nicholson S (1994) Contrasting conditions of surface water balance in wet years and dry years as a possible land surface-atmosphere feedback mechanism in the West African Sahel. J Clim 7:653–668

Miller AJ, Cayan DR, Barnett TP, Graham NE, Oberhuber JM (1994) The 1976–77–climate shift of the Pacific Ocean. Oceanogr 7:21–26

Nicholson SE (2009) A revised picture of the structure of the "monsoon" and land ITCZ over West Africa. Clim Dyn, accepted. doi:10.1007/s00382-008-0514-3

Nicholson SE, Grist JP (2003) The seasonal evolution of the atmospheric circulation over West Africa and equatorial Africa. J Clim 16:1013–1030

Nicholson SE, Webster PJ (2007) A physical basis for the interannual variability of rainfall in the Sahel. Quart J R Met Soc 133:2065–2084. doi:10.1002/qj.104

Paeth H, Friederichs P (2004) Seasonality and time scales in the relationship between global SST and African rainfall. Clim Dyn 23:815–837. doi:10.1007/s00382-004-0466-1

Polo I, Rodríguez-Fonseca B, Losada T, García-Serrano J (2008) Tropical Atlantic variability modes (1979–2002). Part I: time-evolving SST modes related to West African rainfall. J Clim 21:6457–6475. doi:10.1175/2008JCLI2607.1

Ramel R, Gallée H, Messager C (2006) On the northward shift of the West African monsoon. Clim Dyn 26:429–440. doi:10,1007/s00382-005-0093-5

Ritcher I, Mechoso CR, Robertson AW (2008) What determines the position and intensity of the south Atlantic anticyclone in Austral Winter? An AGCM study. J Clim 21:214–229

Robertson AW, Farrara JD, Mechoso CR (2003) Simulations of the atmospheric response to South Atlantic Sea surface temperature anomalies. J Clim 16:2540–2551

Roeckner E, Arpe K, Bengtsson L, Christoph M, Claussen M, Dümenil L, Esch M, Giorgetta M, Schlese U, Schulzweida U (1996) The atmospheric general circulation model ECHAM-4: model descriptions and simulation of present-day climate. Max-Planck-Institute Rep 218, 94 pp, Hamburg, Germany

Rowell DP, Folland CK, Maskel K, Owen JA, Ward MN (1995) Variability of the summer rainfall over tropical North Africa (1906–92): observations and modeling. Quart J Roy Meteor Soc 121:669–704. doi:10.1002/qj.49712152311

Shinoda M, Kawamura R (1994) Tropical rainbelt, circulation and sea surface temperatures associated with the Sahelian rainfall trend. J Meteor Soc Jpn 72:341–357

Smith TM, Reynolds RW (2004) Imporved extended reconstruction of SST (1854–1997). J Clim 17:2466–2477

Sultan B, Janicot S (2000) Abrupt shift of the ITCZ over West Africa and intra-seasonal variability. Geophys Res Lett 27:3353–3356

Sultan B, Janicot S (2003) The West African monsoon dynamics. Part II: The "preonset" and "onset" of the summer monsoon. J Clim 16:3407–3427

Tomas RA, Webster PJ (1997) The role of inertial instability in determining the location and strength of near-equatorial

convection. Quart J Roy Meteor Soc 123:1445–1482. doi: 10.1002/qj.49712354202

Uppala SM et al (2005) The ERA-40 reanalysis. Quart J Roy Meteor Soc 131:2961–3012. doi:10.1256/gj04176

Vizy EK, Cook KH (2001) Mechanisms by which Gulf of Guinea and Eastern North Atlantic Sea surface temperature anomalies can influence African rainfall. J Clim 14:795–821

Vizy EK, Cook KH (2002) Development and application of a mesoscale climate model for the tropics: influence of sea surface temperature anomalies on the West African monsoon. J Geophys Res Atmos 107(D3):4023. doi: 10.1029/2001JD000686

von Storch H, Zwiers FW (1999) Statistical analysis in climate research. Cambridge University Press, New York. ISBN 0521450713

Ward MN (1998) Diagnosis and short-lead time prediction of summer rainfall in tropical North Africa at interannual and multidecadal timescales. J Clim 11:3167–3191

Xie P, Arkin PA (1997) Global precipitation: a 17-year monthly analysis based on gauge observations, satellite estimates, and numerical model outputs. Bull Am Meteor Soc 78:2539–2558

Zebiak SE (1993) Air–sea interaction in the equatorial Atlantic region. J Clim 6:1567–1586